THE ASTROPHYSICAL JOURNAL, 567:1225–1233, 2002 March 10

SOLAR DISAPPEARING FILAMENT INSIDE A CORONAL HOLE

I. M. CHERTOK, E. I. MOGILEVSKY, V. N. OBRIDKO, AND N. S. SHILOVA
IZMIRAN, Troitsk, Moscow Region, 142190, Russia; ichertok@izmiran.troitsk.ru

AND

H. S. HUDSON
Solar Physics Research Corporation, ISAS, Sagamihara-shi, Kanagawa 229, Japan
Received 2001 January 25; accepted 2001 November 9

ABSTRACT

Based on *Yohkoh*/SXT, *SOHO*/EIT images and movies, as well as on Hα, He I 10830 Å heliograms and other relevant data, we analyze an event of 1999 December 28, which is interesting in at least two aspects. (1) A major horseshoe-shaped Hα filament appeared to be located within a large transequatorial coronal hole (CH) in the eastern hemisphere. (2) This filament subsequently disappeared, with its eruption combined with a number of dynamic phenomena, including large-scale ones. The probable location of the filament inside the CH was confirmed in detail by calculations of the open field regions and, for the first time, the quasi-separatrix layers in the global solar magnetic field. The filament eruption was accompanied by significant evolution of the soft X-ray and EUV-emitting structures inside the CH as well as by a coronal mass ejection. The analysis indicates that CHs need not have the simple and uniform structure normally assumed and can sometimes contain local areas with low-altitude closed magnetic fields. It demonstrates also that the erupting filament inside the CH was a part of a much more global, evolving magnetic structure associated with activity extending through at least the entire eastern half of the disk.

Subject headings: Sun: corona — Sun: filaments — Sun: UV radiation

1. INTRODUCTION

It is usually believed that coronal holes (CHs) represent areas of relatively cool, low-density (and hence X-ray faint) plasma with open, predominantly unipolar magnetic fields and without significant internal activity (e.g., Zirker 1977; Harvey 1995; Mogilevsky, Obridko, & Shilova 1997; Obridko & Shelting 1999; Zhao, Hoeksema, & Scherrer 1999). In soft X-rays and high-temperature EUV lines, they are visible as extended structures with diminished emission. They are bright in the He I 10830 Å chromospheric absorption line, modified by overlying coronal radiation with wavelengths smaller than 500 Å and have reduced internal network intensity and contrast. Cold filaments and hot active regions both appear dark.

The most common type of the small-scale activity observed inside CHs appears to be soft X-ray bright points and the corresponding dark points visible in the He I 10830 Å line (e.g., Nolte et al. 1978; Kahler & Moses 1990; Harvey 1995). Among the medium-scale features inside CHs, emerging magnetic fluxes (Stepanyan & Malanushenko 2001) and compact active regions capable of producing large soft X-ray coronal jets (e.g., Shibata et al. 1994) sometimes appear.

In this paper, we present the event of 1999 December 28–29, which is of interest due to two essential peculiarities (Fig. 1). In this case, a reasonably large filament appeared to be located within an extended transequatorial CH. Moreover, a disappearance/eruption of this filament occurred. The disappearance was accompanied by a number of large-scale dynamic phenomena such as a coronal mass ejection (CME), EUV-emitting structures inside the CH, a soft X-ray arcade, and some other effects. These features seem to mean that CH structures need not be so simple and quiet as previously assumed.

In § 2, the data and approach used in the analysis are outlined. Diverse imaging and magnetic field data on the filament position relative to the CH are presented in § 3. As a whole, these data indicate the probable location of the filament inside a CH. The activity preceding the filament eruption, as well as the eruption itself and the accompanying phenomena are described and analyzed in § 4. The discussion and conclusion are given in § 5.

2. DATA AND APPROACH

The majority of the full-disk images and movies used in this analysis are accessible through the Internet. The Hα heliograms of the Big Bear Solar Observatory (BBSO), Mauna Loa Solar Observatory/High Altitude Observatory (MLSO/HAO), and National Astronomical Observatory (Mitaka) are used to search dynamics of the filament. The He I 10830 Å spectroheliograms of the MLSO/HAO and National Solar Observatory (Kitt Peak) allowed us to have information on the visibility, location, and configuration of the CH in this line as well as on the position and evolution of the filament. The imaging data from the *Yohkoh*/SXT (Tsuneta et al. 1991) are known to be valuable material both for locating CHs and observing posteruption structures; for example, arcades.

Observations from the EUV Imaging Telescope (EIT; Delaboudinière et al. 1995) aboard the *Solar and Heliospheric Observatory* (*SOHO*) were also widely used. In particular, the images in the high-temperature (2.0 MK) Fe XV 284 Å line are almost as informative about CHs as the soft X-ray heliograms. Two other coronal lines, Fe IX, X 171 Å and Fe XII 195 Å, sensitive to the coronal plasma with the temperature of 1.1 and 1.5 MK, are the most suitable for detection of the emitting coronal features particularly associated with the filament activity. To make these relatively faint features visible and pronounced, the modified EUV images with a limited range of intensities were formed. On some of them, the brighter sources associated with active regions prove to be saturated. The white-light infor-

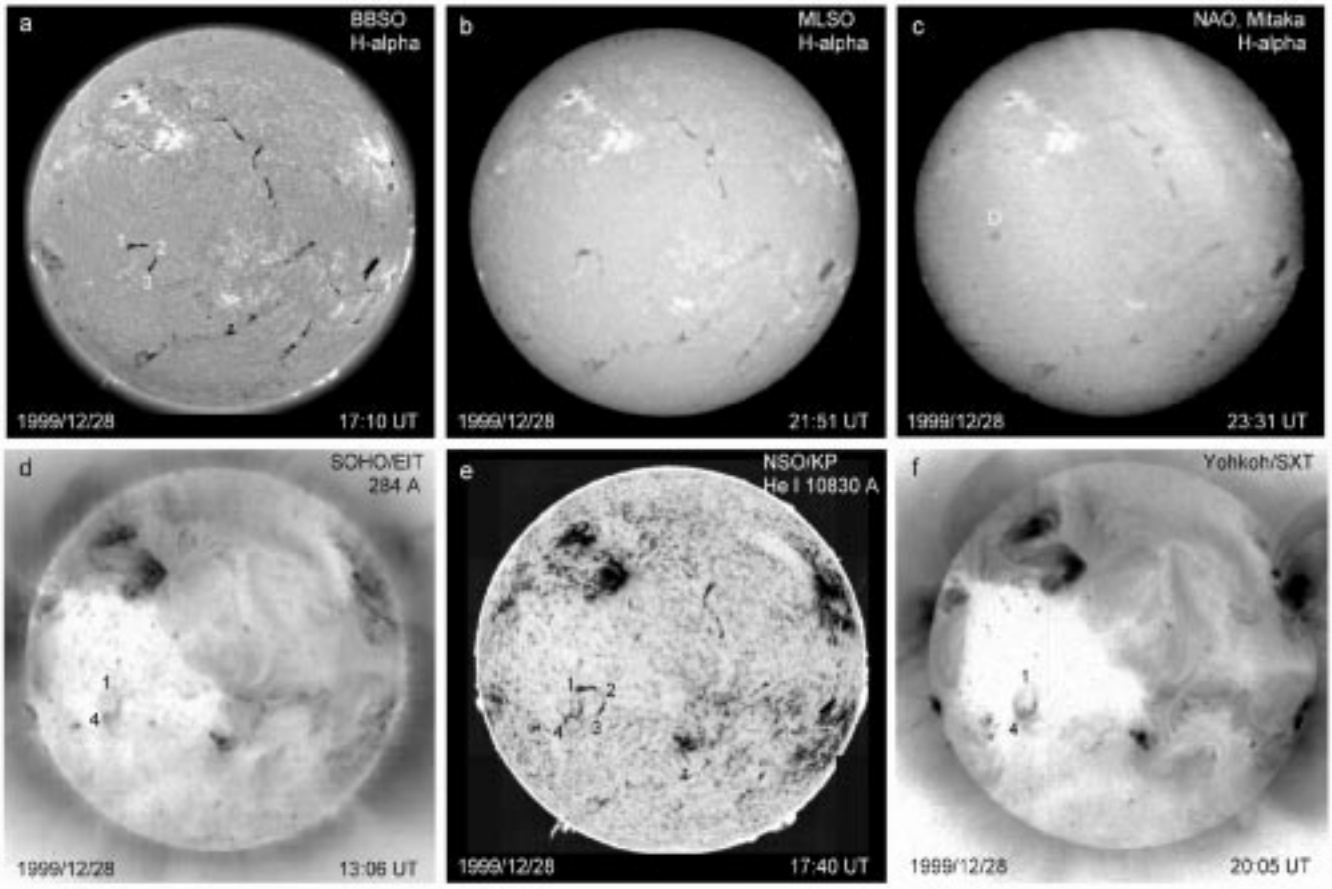

FIG. 1.—*Top row*: BBSO (*a*), MLSO (*b*), and Mitaka (*c*) Hα images of 1999 December 28 illustrating presence, evolution, and disappearance of the horseshoe-shaped filament 1-2-3. Blob D on the frame (*c*) is an artifact. *Bottom row*: Negative modified *SOHO*/EIT 284 Å (*d*) and *Yohkoh*/SXT (*f*) images with the large CH on the eastern half of the disk and inside emitting element 4-1 as well as the positive Kitt Peak He I 10830 Å spectroheliogram (*e*), in which both the filament 1-2-3 and emitting element 4-1 are visible.

mation on CME occurrence comes from the Large Angle Spectroscopic Coronagraph (LASCO; Brueckner et al. 1995) on the *SOHO* spacecraft.

The most complete observations covering the whole event under consideration were made by *SOHO*/EIT at the 195 Å wavelength with a 12-minute cadence. These data indicate that the main filament eruption occurred on December 28 around 22–23 UT. Unfortunately, the available Hα data have a gap just at this time between 21:51 and 23:31 UT. The last MLSO/HAO spectroheliogram in the

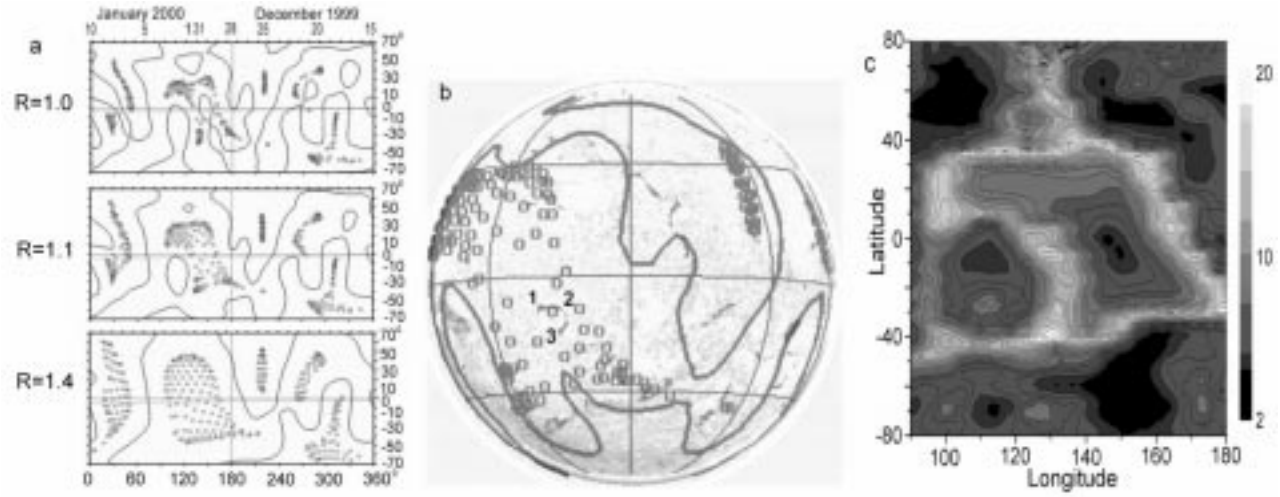

FIG. 2.—(*a*) Calculated synoptic magnetic maps of the radial field at the heliocentric distances of $R = 1.0$, 1.1, and $1.4\,R_\odot$ centered at 1999 December 28. Thick line marks the neutral lines of the large-scale magnetic fields. Small circles are bases of open field lines at each level. (*b*) Projection of the computed synoptic map at $1.1\,R_\odot$ with the open field area on the solar sphere superimposed on the BBSO Hα heliogram (Fig. 1*a*) demonstrating location of the filament 1-2-3 inside the CH, identified with the open field line area. (*c*) Distribution of the footpoint separation factor N on the synoptic chart of the eastern half of the disk at $1.1\,R_\odot$, displaying the QLSs particularly along the CH boundaries.

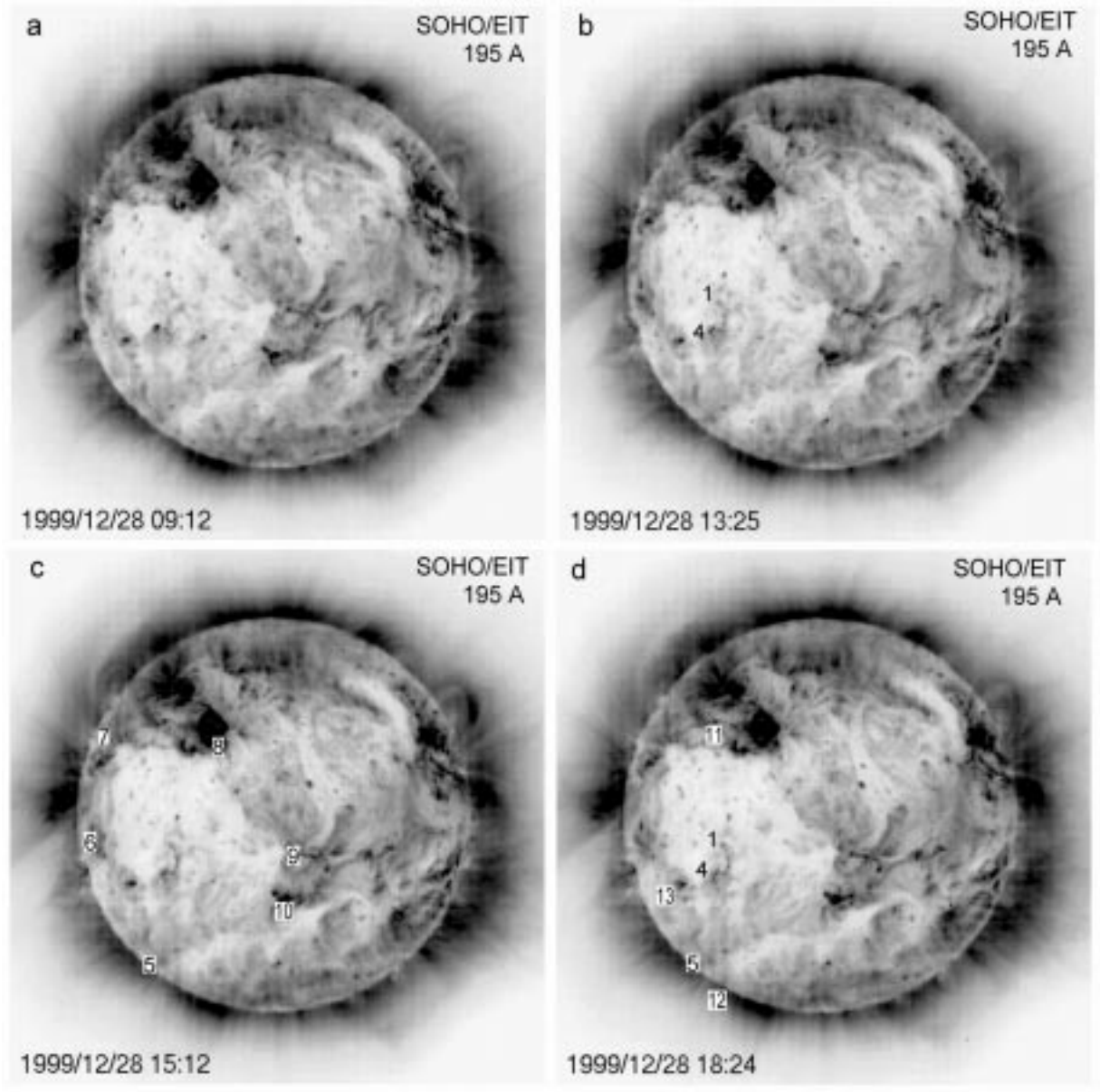

FIG. 3.—Modified *SOHO*/EIT 195 Å images of 1999 December 28 at the pre-eruption stage illustrating development of the inside-CH curved emitting element 4-1, as well as some other emitting features, passing through the filament region and outlining the CH boundaries visible particularly in the 284 Å line and soft X rays (Figs. 1*d* and 1*f*).

He I 10830 Å line was from 22:08 UT, i.e., before the main eruption. Nevertheless, the available multiwavelength data are sufficient to study the peculiar features of the event. It should be kept in mind that in this paper all *Yohkoh*/SXT and *SOHO*/EIT images are presented in the inverted (negative) form, i.e., emitting features appear dark and absorption structures appear bright. At the same time, the Hα, He I 10830 Å, and *SOHO*/LASCO images are shown in the normal (positive) form.

The Stanford digital synoptic magnetic field map for 1999 December 28 and the corresponding IZMIRAN techniques were used to calculate the open field areas and, most interestingly, the quasi-separatrix layers in the global magnetic field (Obridko, Kharshiladze, & Ivanov 2002). These calculations help us to outline the location, configuration, and boundaries of the CH. The short definition and explanation of the quasi-separatrix layers with some relevant references are given in § 3.[1]

3. ON LOCATION OF THE FILAMENT RELATIVE TO THE CORONAL HOLE

In Figures 1*a* and 1*b*, particularly from the Hα heliograms of 1999 December 28, one can see that the horseshoe-shaped filament 1-2-3 of our interest was reasonably long (about 250 Mm) and located in the southeast quadrant. On this day, the clear, large, transequatorial CH, best visible on the *SOHO*/EIT 284 Å (Fig. 1*d*) and *Yohkoh*/SXT (Fig. 1*f*)

[1] Digital versions of the relevant illustrations, including not only figures but also movies in Javascript and MPEG formats, can be found at the following web site: http://helios.izmiran.troitsk.ru/lars/Chertok/991228/title.html.

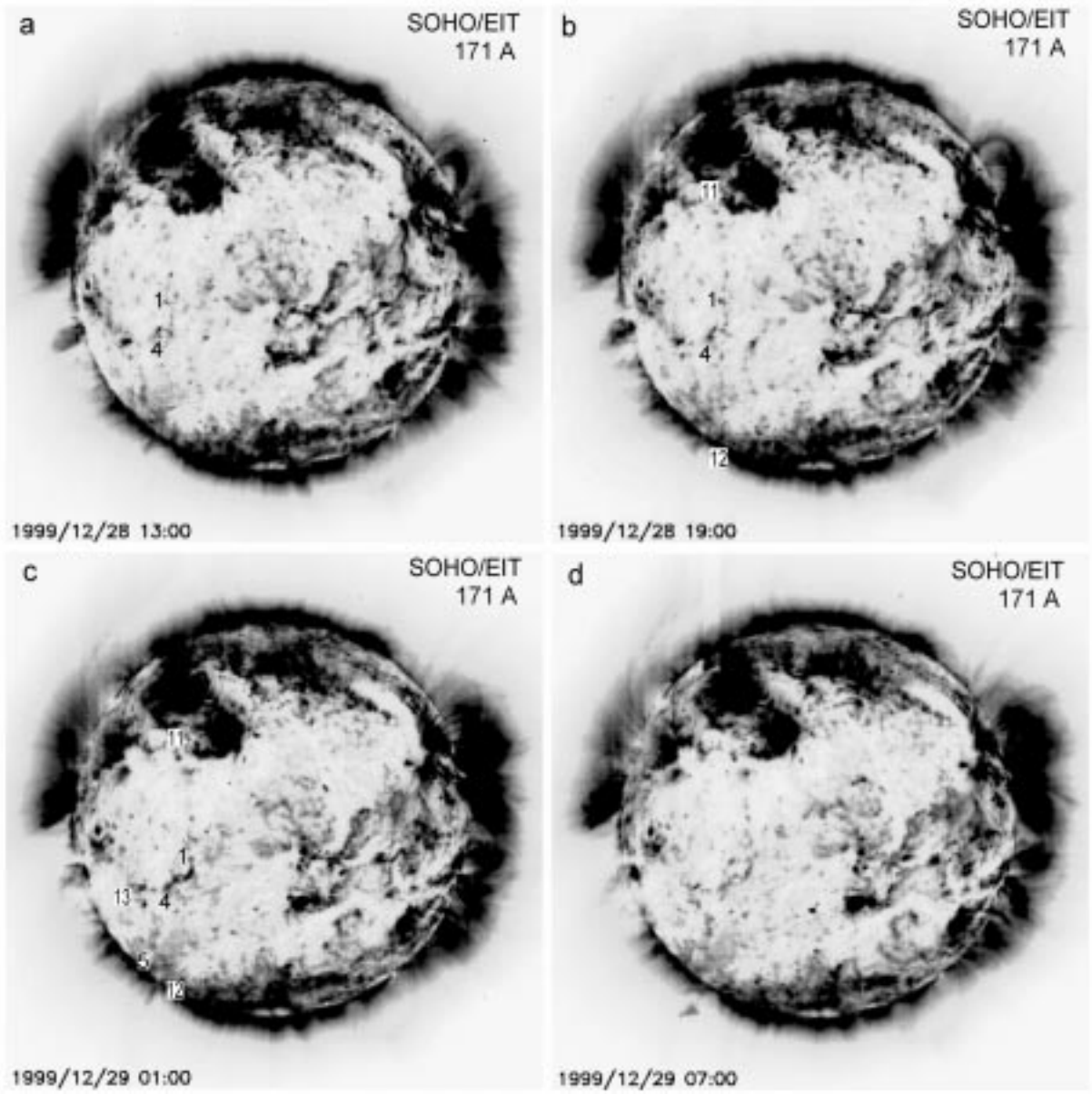

FIG. 4.—Modified *SOHO*/EIT 171 Å images illustrating development of the inside-CH bright element 4-1 and emitting features before filament eruption (*a*, *b*) and at the post-eruption stage (*c*, *d*).

images, is present in the central sector of the eastern half of the disk. On the Kitt Peak He I 10830 Å spectroheliogram (Fig. 1*e*), as well as on the similar MLSO/HAO spectroheliograms (see Fig. 5), the CH and its boundaries are not sharply defined. Nevertheless, it seems that the filament 1-2-3 appears to be located near the southern boundary of the He I 10830 Å CH. It is important to note that the curved emitting element 1-4, visible as dark on the negative *SOHO*/EIT 284 Å (Fig. 1*d*), *Yohkoh*/SXT (Fig. 1*f*) images, and on the positive He I image (Fig. 1*e*), is located southeastward relative to the filament. Taking this point into account, one can conclude from the *SOHO*/EIT 284 Å (Fig. 1*d*) image and especially from the *Yohkoh*/SXT (Fig. 1*f*) images (see also Fig. 6) that the filament 1-2-3 appears to be positioned inside the CH visible in the soft X-rays and high-temperature 284 Å line.

Unfortunately, at present there is no objective or quantitative method for determining the CH boundaries on soft X-ray, EUV, and He I 10830 Å heliograms (e.g., Zhao et al. 1999). The Kitt Peak CH maps routinely published in the Solar-Geophysical Data (SGD) are constructed from the full-disk He I 10830 Å spectroheliograms and magnetograms, based on qualitative criteria (e.g., Recely & Harvey 1986); these criteria exclude a priori any nonunipolar features—particularly filaments—inside CHs. For our case of 1999 December 28 (SGC 2000), the Kitt Peak map classifies as a CH only the "bright" northeastern part of the CH visible on the soft X-ray and 284 Å images as well as two small patches located near the central meridian, in the southeast sector of this CH. The area adjoining the filament 1-2-3 is not included in the CH on the Kitt Peak map. Therefore, one can note that in our case, as well as in some other cases, the He I 10830 Å spectroheliograms display mainly the most intense and pronounced areas of the real CH (see below).

Let us consider now the information on the CH which can be inferred from some magnetic field data. From the physical point of view, perhaps the most reliable and valid

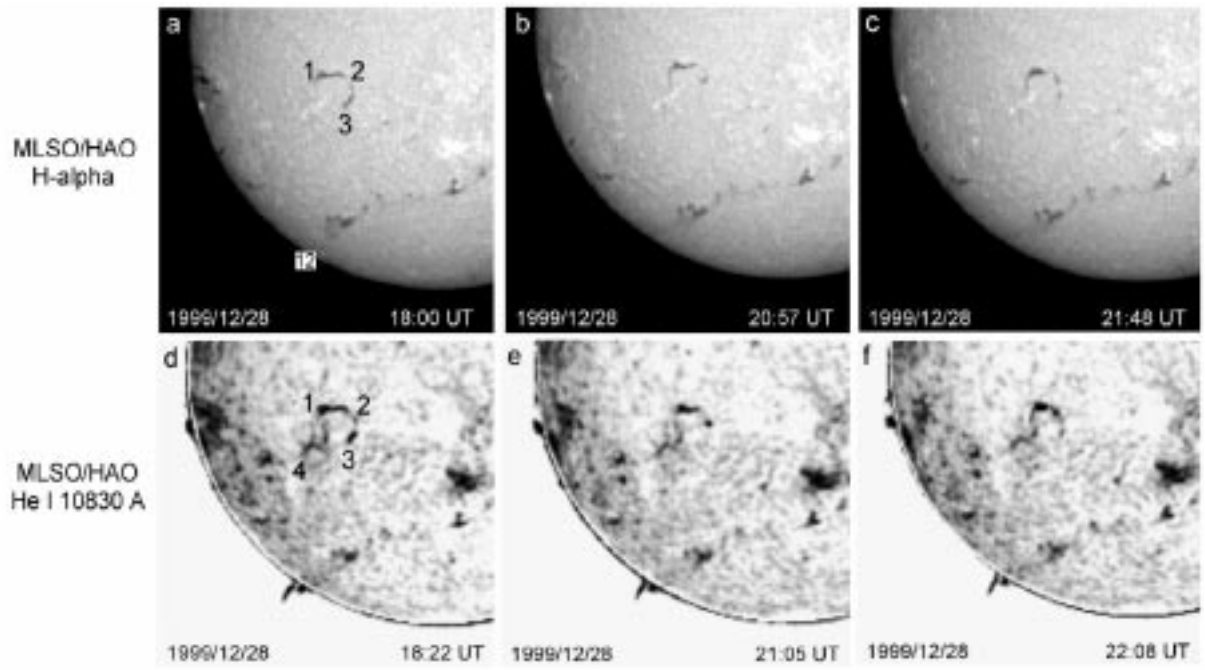

FIG. 5.—Fragments of the MLSO/HAO Hα (*a–c*) and He I 10830 Å (*d–f*) images displaying partial disappearance of the southern branch of the filament 1-2-3 before the main eruption of the whole filament. Adjacent emitting element 4-1 is also visible in the He I line.

approach to determination of a CH configuration is its identification with the computed footpoint area of open field lines (Obridko & Shelting 1999; Zhao et al. 1999). Shown in Figure 2*a* are the synoptic magnetic field maps of the radial field at the heliocentric distances of $R = 1.0$, 1.1, and 1.4 $R_\odot$ calculated using the Stanford synoptic chart and IZMIRAN modification of the potential field-source surface model (Obridko & Shelting 1999; Obridko et al. 2002). All maps are centered at 1999 December 28. The thick lines mark the neutral lines of the large-scale magnetic fields. The small circles are the bases of the open field lines at each level. One can see that the location and configuration of the eastern open field area corresponds well to the CH visible on the soft X-ray and 284 Å images. (Also, the northwest narrow open field region matches another CH in the northwest quadrant.) These data show additionally that the CH under consideration spans a region of complex magnetic field. At the photospheric level, this includes a near-equatorial region of closed field and even a field of opposite polarity. The magnetic field structure, however, simplifies significantly with height and becomes almost simply connected already at $R = 1.1$ $R_\odot$. Figure 2*b* shows the computed synoptic map at $R = 1.1$ $R_\odot$, with the open field area projected on the solar sphere, superimposed on the BBSO Hα heliogram shown in Figure 1*a*. This composite picture demonstrates clearly that the filament 1-2-3 of our interest is really located inside the calculated open field area, i.e., inside the CH at this altitude.

An additional novel aspect of the magnetic field under consideration is the comparison of the CH and other large-scale features with calculated quasi-separatrix layers of the three-dimensional global coronal magnetic fields. According, for example, to Démoulin et al. (1997), Titov (1999), and Titov & Hornig (2001), the quasi-separatrix layers are the regions of drastic change in the field-line linkage formed on the boundaries of different interacting magnetic flux systems. The quasi-separatrix layers are of interest because magnetic reconnection and energy release may occur there.

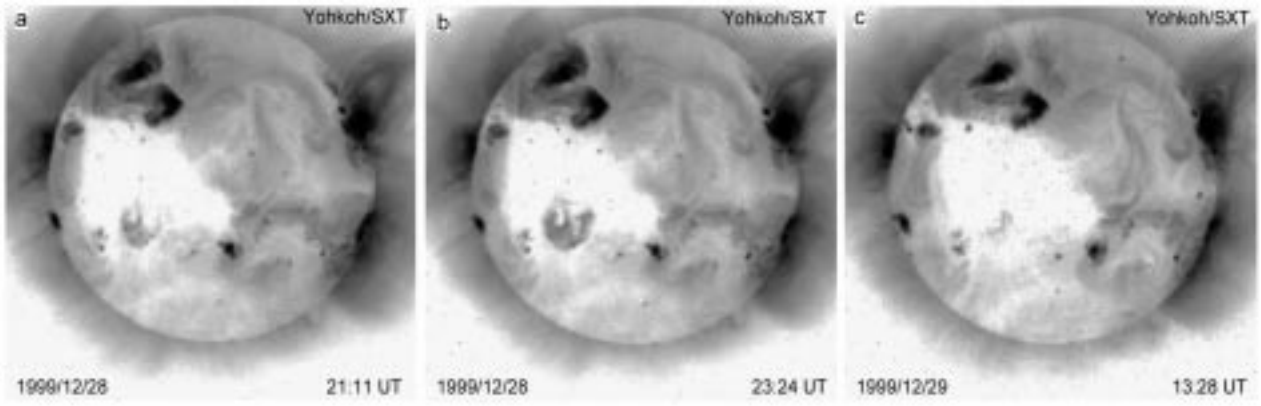

FIG. 6.—*Yohkoh*/SXT images illustrating development of the inside-CH soft X-ray arcade before (*a*), during (*b*), and after (*c*) the main filament eruption. (See also Fig. 1*f*.)

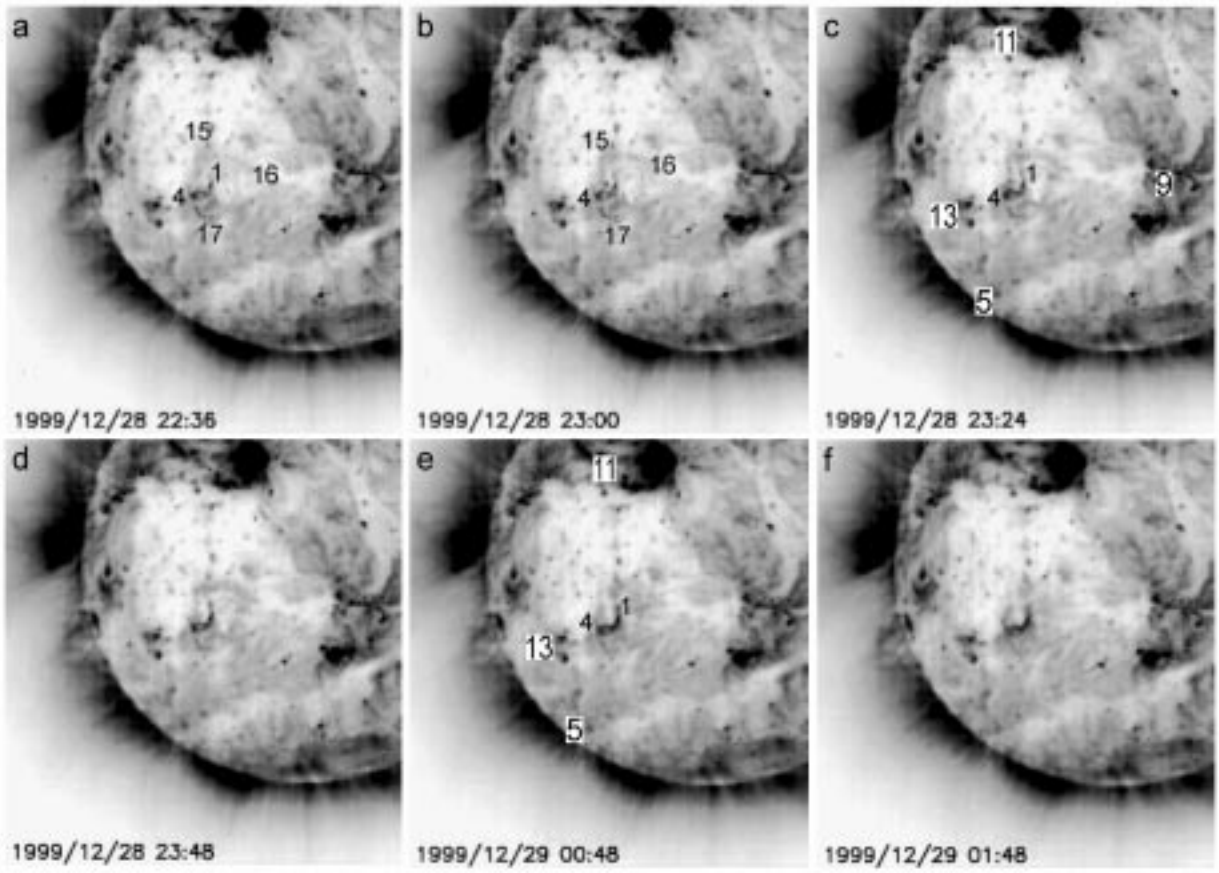

FIG. 7.—Modified *SOHO*/EIT 195 Å images at the eruption (*a–d*) and posteruption (*e–f*) stages illustrating development of curved element 4-1 and oval emitting feature 4-15-16-17-4 around the filament region as well as some other associated emitting structures. (See text.)

So far, the separators, the quasi-separatrix layers, and other similar peculiarities of the three-dimensional magnetic field topology have been modeled for the local magnetic field systems above isolated active regions, where they could be identified with flare-related features and bright loops observed in the Hα, soft X-ray, and EUV ranges (e.g., Gorbachev & Somov 1988; Démoulin et al. 1997; Wang et al. 2000). Now the technique has been further developed in IZMIRAN (Obridko et al. 2002), allowing us to compute large-scale quasi-separatrix layers in the global coronal magnetic field. It is reasonable to expect, in particular, that some quasi-separatrix layers arise on the CH boundaries because here the open and closed magnetic fluxes interact with each other. The location of the quasi-separatrix layers is calculated by the so-called footpoint separation factor N, which characterizes a ratio of the starting point distances of the field lines to their end-point distances. Figure 2*c* shows the spatial distribution of the separation factor N at a heliocentric level of 1.1 $R_\odot$ on the synoptic chart corresponding to the eastern half of the disk of 1999 December 28. It can be seen that the biggest values of the factor N, i.e., the quasi-separatrix layers, outline the boundaries of the large-scale structure, which appears to coincide with the CH, visible in the 284 Å line and soft X-rays shown in Figures 1*d* and 1*f*, as well as with the calculated open field area presented in Figure 2*a*.

Thus, although the position of the filament 1-2-3 relative to the CH on the He I 10830 Å spectroheliograms is questionable, other important data, such as the soft X-ray and 284 Å images, computed open field area, and quasi-separatrix layers indicate the location of the filament inside the CH.

4. MANIFESTATIONS OF THE FILAMENT ERUPTION

Similar to usual filament eruption events occurring outside CHs, in the case under consideration, noticeable activity began long before the eruption. At the 195 Å wavelength (Fig. 3), the bright curved emitting element 4-1, mentioned already in the first paragraph of § 3, develops from bright point 4 near the filament between 09:12 UT (Fig. 3*a*) and 13:25 UT (Fig. 3*b*). During several following hours, this feature continues to develop (Fig. 3*c*) and its intensity increases significantly to 18:24 UT (Fig. 3*d*). Some other emitting features are present in and near the filament area within the CH at this stage. On the 171 Å *SOHO*/EIT pre-eruption images (Fig. 4, *top row*), a similar but somewhat different filament-associated activity, particularly an analog of the near-the-filament emitting curved element 4-1, is visible.

The MLSO/HAO Hα and He I 10830 Å heliograms (Fig. 5) illustrate the pre-eruption evolution of the filament 1-2-3 at the time interval between 18 and 22 UT. The Hα brightening, positioned southeastward of the horseshoe-shaped filament 1-2-3, appears to be a partial counterpart of the curved emitting element 4-1 mentioned above (see also Figs. 1, 3, and 4). Comparison of two pairs of the images (Figs. 5*a* and 5*d* with Figs. 5*b* and 5*e*) shows that an almost absolute disappearance of the southern branch 3-2 of the filament

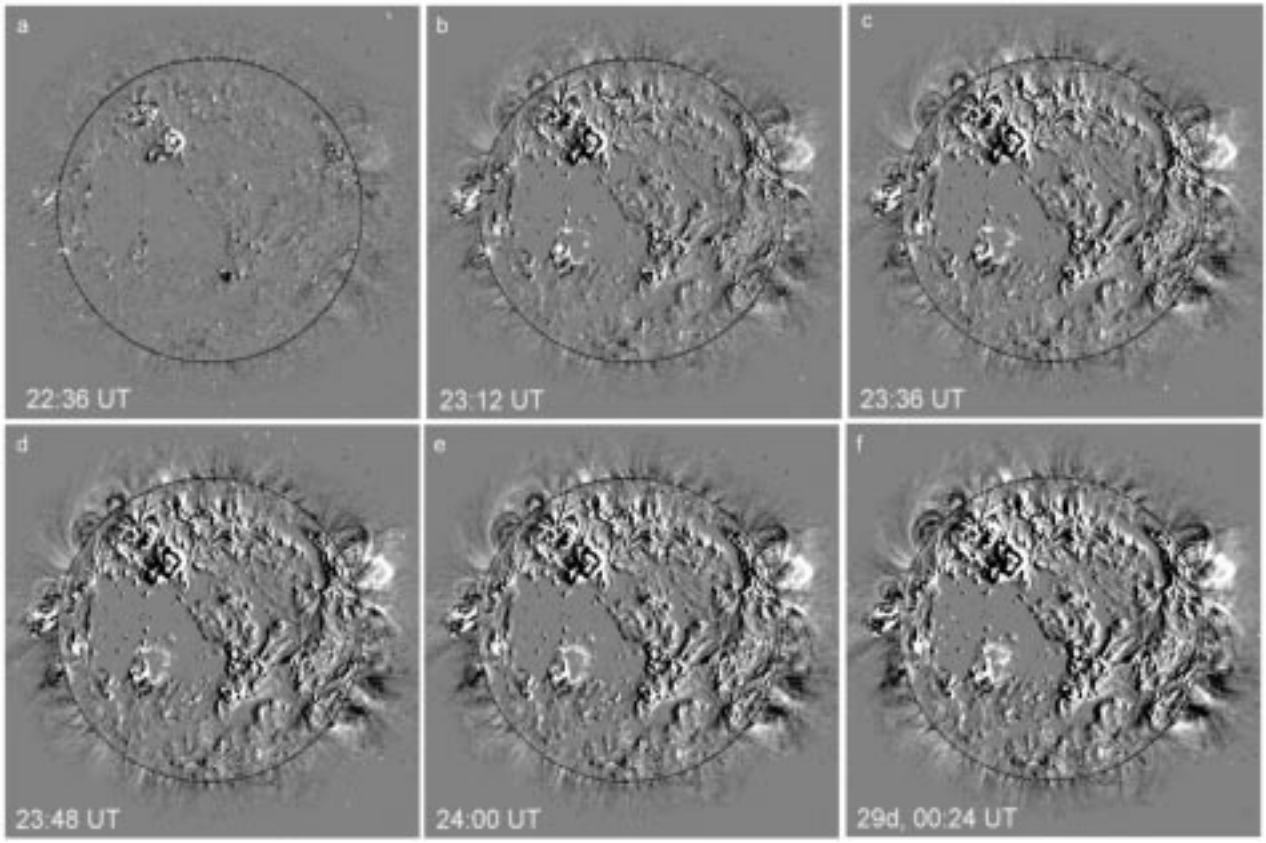

FIG. 8.—Difference (relative to 22:24 UT) *SOHO*/EIT 195 Å images near the eruption stage displaying development of the curved element and oval emitting structure around the eruptive filament within the CH. (See also the caption and numbering of Fig. 7.)

occurred at about of 21 UT in both the Hα and He I 10830 Å ranges. Just at this time, a significant intensification and enlargement of the soft X-ray emission in the near-the-filament region inside the CH takes place (Figs. 1*f* and 6*a*). Nearer to the main eruption time, the southern filament branch 3-2 becomes visible partly again on the Hα and He I images (Fig. 5*c* and 5*f*; see also Fig. 1*b*).

The occurrence of the main eruption of the whole filament at about 23 UT follows not only from a comparison of the nearest of the available Hα heliograms (Figs. 1*b* and 1*c*) but also from the detailed *SOHO*/EIT data at 195 Å (Fig. 7). In addition to the various emitting features appearing southward of the bright curved element 4-1 near point 17, the east (4-15) and north (15-16) diffuse emitting branches are visible at 22:36 UT (Fig. 7*a*). Then at 23:00 UT (Fig. 7*b*), these branches transform rather sharply into a closed, oval, emitting structure 4-15-16-17-4 surrounding the filament region. Simultaneously, a few transient bright points appear near element 4-1. The oval structure remains pronounced and occupies a more or less stable position during at least several tens of minutes (Fig. 7*b*–7*d*), accompanied by some enhancement and swelling of the curved element 4-1. These features of the eruption stage of the event are more prominently visible on the *SOHO*/EIT 195 Å difference

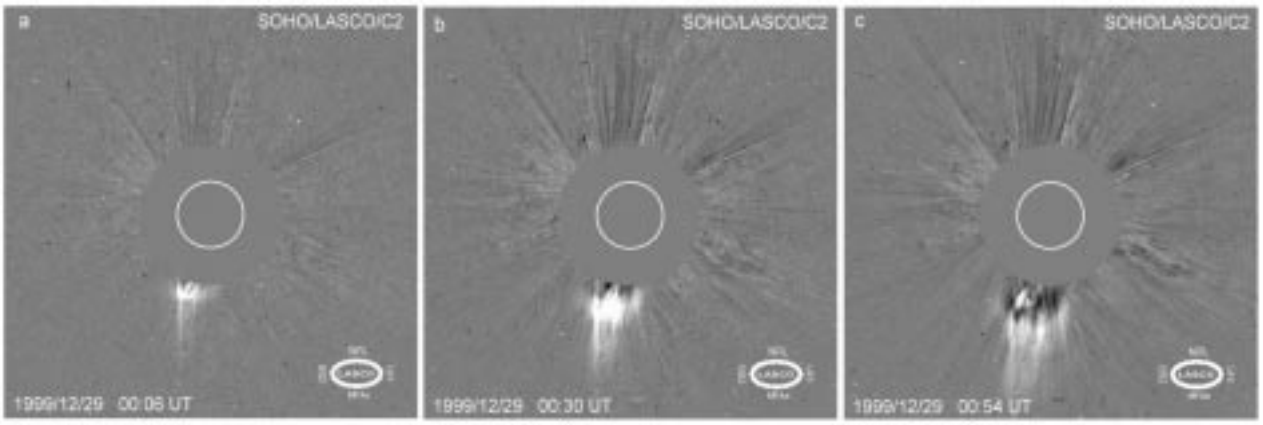

FIG. 9.—Running difference *SOHO*/LASCO images of 1999 December 29 displaying the southeastern CME associated with the CH filament eruption. (Courtesy of S. Plunkett.)

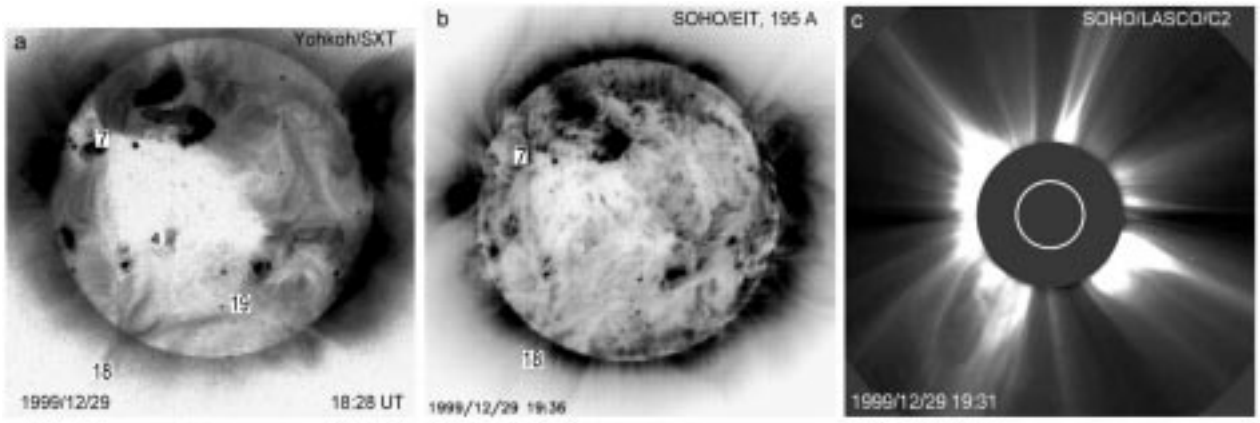

FIG. 10.—Phenomena accompanying the eruption of the southeast filament (see Fig. 1*a*–1*c* and Fig. 5) on 1999 December 29. (*a*) Huge soft X-ray cusp structure 18 with three legs extending to the northeast region 7 along the eastern CH boundary to the still-illuminated inside-CH filament area 4 and some southward of the erupted south filament 19. (*b*) 195 Å counterparts of these structures. (*c*) Southeast CME registered with the *SOHO*/LASCO.

images (Fig. 8), where the 22:24 UT image was used as a background. It is reasonable to note that the CH, coinciding with the soft X-ray and 284 Å one, is clearly distinguished on these images.

In soft X-rays, the filament eruption manifested itself by significant intensification and development of an arcade-like structure (Fig. 6*b*). It is essential that this large-scale structure also occurred inside the soft X-ray CH and was located mainly south-southeast relative to the filament region, consistent with the projection of the local vertical. It seems that this direction was somewhat distinguished, because according to the *SOHO*/LASCO data (Fig. 9), a rather noticeable CME was observed just over the south-southeastern limb after 23:30 UT. By our estimation, at the heliocentric distance range of 2.5–7.0 $R_{\odot}$, the projected velocity of the CME increased from 270 to 520 km s^{-1}. It is reasonable to suggest that this CME was associated with the filament erupted from within the CH under consideration.

During all phases of the event, i.e., before, at the time of, and after the filament eruption on the 195 Å images, one can see some thin emitting structures outlining the area, corresponding to the CH observed in soft X-rays and 284 Å (see, for example, the contour 5-6-7-8-9-10-5 in Fig. 3*c*). According to the findings of Chertok (1999, 2001), these so-called large-scale chains are observed rather often, particularly at the boundaries of CHs. It should be noted that in this case, the CH boundary-associated chains appear to coincide also with the calculated quasi-separatrix layers of the global coronal magnetic fields (Fig. 2*c*). Such an association of the chains with energy release in large-scale quasi-separatrix layers was supposed by Chertok (1999, 2001). One more meridional transequatorial chain was observed at both 171 and 195 Å lines and passed through the filament region 1-4 inside the CH extending at first (Figs. 3*d* and 4*b*) from environs of the northeastern active complex 11 and then (Figs. 4*c*, 4*d*, and 7*f*) to the southeastern CH boundary 13-5 and to the southeast limb edge 12 of the long south filament visible in the Hα and He I 10830 Å lines (see Figs. 1 and 5). This filament-associated transient chain seems to resemble the patchy ribbons observed particularly in the He I 10830 Å line on either side of the channel from which a filament has erupted (e.g., Harvey et al. 1987, 1996). The development of the chains in the event under consideration will be discussed in more detail in a separate paper.

The large-scale features described above suggest a close physical connection between the CH, the filament interior to it, the neighboring active region complexes 9 and 11, and the southeastern filament region 5 (e.g., Figs. 3, 4, and 7). The illumination and development of the large-scale emitting structures, particularly going to the southeastern limb, indicate strong evolution of this part of the global solar magnetic fields. It appears not to be a coincidence that on December 29 at about 15 UT, the southeastern filament also erupted. This resulted in a relatively large, very slow (182 km s^{-1}), loop-like CME (Fig. 10*c*) as well as the huge over-the-limb soft X-ray cusp structure (18) with three diffuse, leg branches (Fig. 10*a*). One leg, 18-7, visible also at 195 Å (Fig. 10*b*), extends to the northeastern region along the east CH boundary, the second (18-4) stretches to the still-illuminated filament area within the CH, and the third (18-19) is positioned along but somewhat southward of the southern erupted filament. This implies close connections existing between all these structures and tends to confirm their involvement in the large-scale eruptive events considered.

5. DISCUSSION AND CONCLUSION

Our multirange analysis of the event of 1999 December 28–29 demonstrates that sometimes large CHs may differ from usual ones with respect to the presence of such internal large-scale activity as a moderately long and eruptive filament.

A number of arguments speak well of the probable location of the filament inside the CH inferred at the heliocentric distance 1.1 $R_{\odot}$. Although their relative position on the Kitt Peak and MLSO/HAO He I 10830 Å images is debatable, the *Yohkoh*/SXT and *SOHO*/EIT 284 Å heliograms clearly show the filament lying within the CH. This conclusion is confirmed also by calculations of two characteristics of the large-scale magnetic fields outlining particularly the CH boundaries: the open magnetic field line area and, for the first time, the quasi-separatrix layer patterns of the global coronal magnetic fields.

The inferred probable location of the filament inside the CH means that some CHs may not be so simple and

uniform a structure as normally believed and can contain local areas of closed large-scale magnetic fields, at least at low altitudes. If the CH is to remain unipolar, another possible interpretation is that the filament and the bipolar region which it separates carve out an interior hole of more complicated magnetic topology that is not a part of the CH.

The fact that this filament within a CH also erupted is one more peculiarity of the event under consideration. Noticeable pre-eruption filament activity, typical for usual filament eruptions occurring outside CHs, was observed in this case as well. The main eruption of the whole filament was accompanied by an obvious white-light CME, an appreciable restructuring of the EUV emission over the large area around the filament, a remarkable soft X-ray brightening and arcade formation, and some other phenomena.

The observed features of the event suggest that the CH, internal and external filaments, and adjacent active regions are combined into a united large-scale active complex extending almost throughout the whole eastern half of the disk. The conception of such large-scale active complexes connected by large-scale magnetic fields was suggested by Mogilevsky et al. (1997). In our case, the observations show that a filament internal to a CH can play an important role in an evolving large-scale active complex, indicated above, and that all components of the complex were strongly involved in the pre-eruption activity, the eruption itself, and post-eruption processes.

At last, consideration of the *Yohkoh*/SXT and *SOHO*/EIT data for other periods shows that similar but not so spectacular CH-interior filaments and extended accompanying activity can be found in some other events.

The authors thank the anonymous referees for their valuable remarks, comments, and suggestions. We are grateful to members of the *SOHO*/EIT and LASCO, *Yohkoh*/SXT, MLSO/HAO, BBSO, NAO (Mitaka), and NSO (Kitt Peak) teams for solar images and movies used in this study. We especially thank Simon Plunkett for the LASCO running difference movie of the CME, as well as Yoshinori Suematsu and Andrew Stanger for the additional Mitaka and MLSO Hα images. The helpful consultations of Roman V. Gorgutsa and Victor V. Grechnev on the computer processing of various solar data are also acknowledged. This work was supported by the Russian Foundation of Basic Research (RFBR), the Russian Federal Program on Astronomy, and the INTAS/RFBR grant for the Joint Research Project on Support for the *SOHO* Solar Maximum Science Mission.

REFERENCES

Brueckner, G. E., et al. 1995, Sol. Phys., 162, 357
Chertok, I. M. 1999, in Proc. 8th *SOHO* Workshop, ed. J.-C. Vial & B. Kaldeich-Schürmann (ESA SP-446; Noordwijk: ESA), 229
———. 2001, Sol. Phys., 198, 367
Delaboudinière, J.-P., et al. 1995, Sol. Phys., 162, 291
Démoulin, P., Bagala, L. G., Mandrini, C. H., Henoux, J. C., & Rovira, M. G. 1997, A&A, 325, 305
Gorbachev, V. S., & Somov, B. V. 1988, Sol. Phys., 117, 77
Harvey, K. L. 1995, in ASP Conf. Ser. 111, Magnetic Reconnection in the Solar Atmosphere, ed. R. D. Bentley & J. T. Mariska (San Francisco: ASP), 9
Harvey, K. L., McAllister, A., Hudson, H., Alexander, D., Lemen, J. R., & Jones, H. P. 1996, in ASP Conf. Ser. 95, Solar Drivers of Interplanetary and Terrestrial Disturbances, ed. K. S. Balasubramaniam, S. L. Keil, & R. N. Smartt (San Francisco: ASP), 100
Harvey, K. L., Sheeley, N. R., Jr., & Harvey, J. W. 1987, in Proc. Solar Terrestrial Predictions Workshop, ed. P. A. Simon, G. Heckman, & M. A. Shea (Boulder: NOAA), 198
Kahler, S. W., & Moses, D. 1990, ApJ, 362, 728
Mogilevsky, E. I., Obridko, V. N., & Shilova, N. S. 1997, Sol. Phys., 176, 107
Nolte, J. T., Davis, J. M., Gerassimenko, M., Krieger, A. S., Solodyna, C. V., & Golub, L. 1978, Sol. Phys., 60, 143
Obridko, V. N., Kharshiladze, A. F., & Ivanov, K. G. 2002, in preparation
Obridko, V. N., & Shelting, B. D. 1999, Sol. Phys., 187, 185
Recely, F., & Harvey, K. L. 1986, Solar-Terrestrial Predictions, ed. P. A. Simon, G. Heckman, & M. A. Shea (Boulder: NOAA), 204
Shibata, K., Nitta, N., Strong, K. T., Matsumoto, R., Yokoyama, T., Hirayama, T., Hudson, H., & Ogawara, Y. 1994, ApJ, 431, L51
Solar-Geophysical Data 2000, Part I. (Boulder: NOAA), 666, 86
Stepanyan, N. N., & Malanushenko, E. V. 2001, Izv. Krimskoi Astrofiz. Obs., 97, 63
Titov, V. S. 1999, Bull. Russian Acad. Sci. & Phys., 63, 1497
Titov, V. S., & Hornig, G. 2001, Adv. Space Res., in press
Tsuneta, S., et al. 1991, Sol. Phys., 136, 37
Wang, H., Yan, Y., Sakurai, T., & Zhang M. 2000, Sol. Phys., 197, 263
Zhao, X. P., Hoeksema, J. T., & Scherrer, P. N. 1999, J. Geophys. Res., 104, 9735
Zirker, J. B., ed. 1977, Coronal Holes and High-Speed Wind Streams (Boulder: Colorado Associated Press)